

# Propofol-induced unresponsiveness is associated with impaired feedforward connectivity in cortical hierarchy

R. D. Sanders<sup>1,\*</sup>, M. I. Banks<sup>1</sup>, M. Darracq<sup>1</sup>, R. Moran<sup>4</sup>, J. Sleigh<sup>5</sup>, O. Gosseries<sup>6</sup>, V. Bonhomme<sup>7,8,10</sup>, J. F. Bricchant<sup>8</sup>, M. Rosanova<sup>11</sup>, A. Raz<sup>1,12</sup>, G. Tononi<sup>2</sup>, M. Massimini<sup>11</sup>, S. Laureys<sup>6,9</sup> and M. Boly<sup>2,3</sup>

<sup>1</sup>Department of Anesthesiology, University of Wisconsin, Madison, WI, USA, <sup>2</sup>Department of Psychiatry, University of Wisconsin, Madison, WI, USA, <sup>3</sup>Department of Neurology, University of Wisconsin, Madison, WI, USA, <sup>4</sup>Faculty of Engineering, University of Bristol, Bristol, UK, <sup>5</sup>Department of Anaesthesia, Waikato Hospital, Hamilton, New Zealand, <sup>6</sup>Coma Science Group, GIGA-consciousness, University of Liège, Liège, Belgium, <sup>7</sup>Anesthesia and Intensive Care Laboratory, GIGA-Consciousness, University of Liège, Liège, Belgium, <sup>8</sup>Department of Anesthesia and ICM, CHU Liège, Liège, Belgium, <sup>9</sup>Department of Neurology, CHU Liège, Liège, Belgium, <sup>10</sup>University Department of Anesthesia and ICM, CHR Citadelle, Liège, Belgium, <sup>11</sup>Department of Biomedical and Clinical Sciences, University of Milan, Milan, Italy and <sup>12</sup>Rambam Healthcare Campus, Haifa, Israel

\*Corresponding author. E-mail: [robert.sanders@wisc.edu](mailto:robert.sanders@wisc.edu)

## Abstract

**Background:** Impaired consciousness has been associated with impaired cortical signal propagation after transcranial magnetic stimulation (TMS). We hypothesised that the reduced current propagation under propofol-induced unresponsiveness is associated with changes in both feedforward and feedback connectivity across the cortical hierarchy. **Methods:** Eight subjects underwent left occipital TMS coupled with high-density EEG recordings during wakefulness and propofol-induced unconsciousness. Spectral analysis was applied to responses recorded from sensors overlying six hierarchical cortical sources involved in visual processing. Dynamic causal modelling (DCM) of induced time–frequency responses and evoked response potentials were used to investigate propofol's effects on connectivity between regions. **Results:** Sensor space analysis demonstrated that propofol reduced both induced and evoked power after TMS in occipital, parietal, and frontal electrodes. Bayesian model selection supported a DCM with hierarchical feedforward and feedback connections. DCM of induced EEG responses revealed that the primary effect of propofol was impaired feedforward responses in cross-frequency theta/alpha–gamma coupling and within frequency theta coupling (F contrast, family-wise error corrected  $P < 0.05$ ). An exploratory analysis (thresholded at uncorrected  $P < 0.001$ ) also suggested that propofol impaired feedforward and feedback beta band coupling. *Post hoc* analyses showed impairments in all feedforward connections and one feedback connection from parietal to occipital cortex. DCM of the evoked response potential showed impaired feedforward connectivity between left-sided occipital and parietal cortex (T contrast  $P = 0.004$ , Bonferroni corrected).

**Editorial decision:** 11 July 2018; **Accepted:** 11 July 2018

© 2018 British Journal of Anaesthesia. Published by Elsevier Ltd. All rights reserved.  
For Permissions, please email: [permissions@elsevier.com](mailto:permissions@elsevier.com)

**Conclusions:** Propofol-induced loss of consciousness is associated with impaired hierarchical feedforward connectivity assessed by EEG after occipital TMS.

**Keywords:** general anesthesia; connectivity; consciousness; electroencephalography; transcranial magnetic stimulation

### Editor's key points

- Cortical connectivity is reduced under general anaesthesia regardless of anaesthetic drug used, which is thought to be attributable mainly to suppression of feedback connectivity.
- This was analysed using transcranial magnetic stimulation coupled with high-density EEG recordings during wakefulness and propofol-induced unconsciousness.
- Dynamic causal modelling showed that the primary effect of propofol was on feedforward connectivity, with some effect on feedback connectivity.
- Thus changes in both feedforward and feedback cortical connectivity might be involved in the effects of anaesthetics on consciousness.

Impaired consciousness has been associated with impaired cortical signal propagation and complexity of cortical responses to transcranial magnetic stimulation (TMS).<sup>1–5</sup> Complexity of the TMS response is preserved with disconnected consciousness<sup>6</sup> or dreaming during ketamine-induced unresponsiveness<sup>5</sup> but not during loss of consciousness with propofol-induced unresponsiveness.<sup>5</sup> These effects might reflect impaired integration of information within the thalamo-cortical system.<sup>7</sup> Consciousness (defined as ‘subjective experience’) results from continuous bidirectional causal interactions between hierarchically organised thalamo-cortical areas.<sup>7,8</sup> We use the term ‘feedback’ to refer to connections from higher- to lower-order brain regions and ‘feedforward’ the opposite, that is connections organised in the same centripetal direction as sensory pathways. Accumulating data show that cortical connectivity is reduced under general anaesthesia, regardless of anaesthetic drug used,<sup>9–16</sup> with evidence from resting state data (collected in the absence of overt sensory stimuli) that feedback connectivity is predominantly suppressed (but see one study with propofol<sup>17</sup>). Moreover, our recent study in rodents found direct evidence that feedback cortico-cortical connections are preferentially suppressed by isoflurane.<sup>18</sup> However, these observations seem at apparent odds with the impaired current propagation observed across the cortex after TMS that would also recruit feedforward pathways, especially if targeted to a lower-order cortical region. We hypothesised that recruiting both feedforward and feedback projections through TMS of sensory cortex would reveal impairment in bidirectional connectivity. We study feedforward and feedback signalling at the cortical level and this should be differentiated from ‘bottom-up’ arousal<sup>19</sup> and sensory signalling<sup>20</sup> that would be recruited more readily by sensory stimuli. Use of TMS is particularly advantageous in this setting, as it allows us to directly perturb cortical dynamics, bypassing ‘bottom-up’ mechanisms, and allowing direct assessment of feedforward and feedback hierarchical interactions of cortex.

The concept of a cortical hierarchy, introduced by Hubel and Wiesel,<sup>21,22</sup> is proposed to underlie an ascending information processing stream, with lower-order sensory regions converging on increasingly complex multimodal association cortices. This has been further developed with models based on predictive coding<sup>23,24</sup> that emphasise the role of descending connections in the integration of information across functionally specialised brain regions. Using TMS to stimulate a lower level of the hierarchy affords the opportunity to model bidirectional connectivity between different levels of the cortical hierarchy.

To provide a mechanistic account of these effects, we used dynamic causal modelling (DCM)<sup>25</sup> to investigate changes in feedforward and feedback connectivity across the cortical hierarchy during propofol-induced unconsciousness. DCM analyses causal interactions among cortical regions, allowing inferences about the strength of feedforward and feedback connectivity and to investigate how directional connectivity changes between experimental conditions. DCM combines realistic dynamical models of interacting cortical regions with a spatial forward model of how cortical activity translates into scalp EEG. This allows estimation of cortical connectivity from observed scalp EEG data within a unified Bayesian framework.

As a limited number of prior sources can be modelled by DCM, herein we selected sources that have been identified previously to be hierarchically connected<sup>26,27</sup> and plausibly involved in generating EEG responses to TMS. Our primary outcome was DCM for induced responses,<sup>25</sup> as it allows modelling of cross-frequency coupling that is important for information transfer across the cortical hierarchy.<sup>23,28</sup> We previously used DCM to model resting-state EEG data between two higher-order cortical regions (finding impaired feedback connectivity)<sup>16</sup>; herein we extend these models to include an additional (lower) level of the cortical hierarchy. DCM offers several advantages for testing hypotheses about between- and within-region coupling, including the use of Bayesian model selection (BMS) to choose the most plausible model for the data.<sup>25</sup> In addition, DCM applied to time–frequency EEG responses allows estimates of between-region ‘within frequency’ and ‘cross-frequency’ coupling, which are all thought to be important for the integration of information between hierarchical regions of cortex. Regarding the latter point, most studies of connectivity between different cortical regions under anaesthesia have focused on ‘within frequency’ effects (e.g. Lee and colleagues,<sup>12</sup> Blain-Moraes and colleagues<sup>29</sup>). Cross-frequency coupling has been shown to play a role in neuronal computation, underlying various cognitive functions including sensory processing, motor responses, and memory, which have relevance for anaesthesia.<sup>30</sup> We focus on the *induced response* that includes power changes that are not necessarily ‘phase locked’ to the stimulus. In contrast, evoked responses are averaged in the time domain before further analyses and so are ‘phase locked’ (the EEG signal has the same phase angle at the start of each trial) to the stimulus. DCM for induced responses

models time-varying spectral changes and the interaction between these spectra at different sources. Essentially this provides assessment of power-based connectivity strengths between multiple sources over time, including the ability to look at cross-frequency power interactions (i.e. amplitude–amplitude coupling). It is important for the reader to note that this is different to other forms of cross-frequency coupling, which are also biologically important, and typically have been assessed using phase–phase or phase–amplitude coupling rather than power coupling.<sup>25,29–33</sup> We also applied DCM to the evoked response potential (ERP), focusing on time domain data rather than time–frequency responses. DCM for ERPs use a cortical neural mass model that explains source activity in terms of the dynamics of interacting inhibitory and excitatory subpopulations of neurones within a cortical source and asymmetric feedforward and feedback interactions between sources. In doing so, we sought to verify the changes that we observed in the DCM of induced responses with those of an alternate, biologically plausible model applied to ERPs.

## Methods

This study was approved by the Ethics Committee of the Medical School of the University of Liege. After informed consent was obtained, eight subjects underwent occipital gyrus (BA19) TMS-EEG ( $\sim 110 \text{ V m}^{-1}$ ) during wakefulness while lying on the bed with eyes open. In a second recording session, a target-controlled infusion (TCI; Alaris TIVA, CareFusion) of propofol was then commenced by a certified anaesthesiologist. Propofol was infused until the subject became unresponsive to verbal command or mild shaking (Ramsay sedation scale 5–6<sup>32</sup>) as with our previous studies of propofol sedation.<sup>5,33</sup> Depth of sedation was assessed using Ramsay sedation scale at 5 min intervals. The initial target for induction was set at  $3 \mu\text{g ml}^{-1}$ , and further adjusted to achieve a Ramsay sedation score of 5 or 6 in all subjects with the lowest propofol concentration. Once the desired level of sedation was obtained, a 5 min equilibration period was allowed to ensure equilibration of propofol concentration between compartments before starting TMS and EEG recording. The propofol concentration needed to achieve a Ramsay score of 5 ranged between 1.8 and  $5 \mu\text{g ml}^{-1}$ . In three subjects additional data were collected at Ramsay sedation scale 3 during induction of anaesthesia, again maintained at a stable plasma concentration with Marsh model TCI. Plasma and effect-site concentrations of propofol were estimated using a three-compartment model<sup>34</sup> and were increased at  $\sim 1 \mu\text{g ml}^{-1}$  increments until unresponsiveness was obtained, with 5 min allowed for equilibration between each change in infusion rate. TMS-EEG was then repeated in this unresponsive state. Throughout the experiment, oxygen was administered through a loosely fitted facemask. None of the subjects recalled events after recovery from propofol-induced unresponsiveness.

TMS was combined with a magnetic resonance-guided navigation system (NBS) and a 60-channel TMS-compatible EEG amplifier (Nexstim eXimia; Nexstim Plc., Helsinki, Finland). Real-time navigation based on individual structural magnetic resonance images was used to optimise the efficacy of TMS targeting the left middle occipital gyrus. The maximum electric field induced by TMS was always oriented perpendicularly to the convexity of the occipital cortical gyrus with intensity adjusted to values above the threshold for a significant EEG response ( $80\text{--}160 \text{ V m}^{-1}$ ). Reproducibility of the stimulation-coordinates across sessions was optimised by software coupled to the NBS

system that indicated in real time any deviation from the desired target,  $>3 \text{ mm}$ . TMS was performed by means of a Focal Bipulse 8-Coil, driven by a Mobile Stimulator Unit (Eximia TMS Stimulator, Nexstim Plc.). At least 200 stimuli were acquired, with stimuli delivered at random intervals (between 2 and 2.3 s). The auditory response to the coil's click and bone conduction were minimised by presentation of white noise while wearing ear plugs.<sup>35</sup> Occipital TMS in wakefulness did not induce reports of changes in visual perception.

## Preprocessing

EEG data were filtered at 0.5–40 Hz (finite impulse response; EEGLAB, Swartz, Center for Computational Neuroscience, University of San Diego, San Diego, USA). Higher frequencies were not analysed over concern of electromyographic contamination of the signal after TMS. Wakefulness and unresponsiveness data were then downsampled to 250 Hz, epoched (from  $-800$  to  $+800 \text{ ms}$  around TMS pulse), and referenced to average using Statistical Parametric Mapping software (SPM12, [www.fil.ion.ucl.ac.uk/spm](http://www.fil.ion.ucl.ac.uk/spm)). For descriptive purposes, we divided data into the following bands: theta 4–8 Hz, alpha 8–14 Hz, beta 14–28 Hz, and gamma 28–40 Hz.

Time–frequency analyses of induced and evoked power were conducted in sensor space for six selected channels in occipital (PO3, PO4), parietal (CP3, CP4), and frontal (AF1, AF2) regions. These regions were selected as overlying hierarchical-connected regions of cortex. For induced power, time domain data underwent time–frequency decomposition using a seventh-order Morlet wavelet transform, and then this time–frequency decomposition was robust averaged. For evoked power, time domain data were robust averaged and then underwent time–frequency decomposition using a seventh-order Morlet wavelet transform.

## Statistical analysis of sensor data

Illustrative group level contrasts were conducted at each channel for changes in the spectral response to TMS induced by propofol using paired T contrasts over 1 Hz frequency bins. Statistical significance was set using a family-wise error (FWE) rate corrected for multiple comparisons either at  $P < 0.05$  at the cluster level (with uncorrected  $P$  value threshold  $< 0.001$ ) or at  $P < 0.05$  at the peak level. As this was a descriptive analysis, cluster FWE is reported when peak FWE is not reached. Note, this is not conducted for the DCM analyses (primary outcome) where only peak FWE is reported.

## Dynamic causal modelling

Because of inherent temporal resolution limitations of time–frequency decomposition, differences in cortico-cortical connectivity are best addressed using model-based approaches such as DCM, which are designed to assess changes in directional (feedforward vs feedback) dynamics that are most likely to explain differences in scalp EEG responses triggered by TMS. Hence we complemented scalp-level analysis with a formal assessment of hierarchical connectivity using DCM that can be divided into two classes: biophysical or phenomenological.<sup>31</sup> Biophysical models (e.g. for ERP) include constraints imposed on the biology of the underlying neuronal circuits such as membrane properties of pyramidal cells or interneurons. Phenomenological models (e.g. for induced responses) describe the statistical relationships between factors

in the model; for induced responses, the critical factors are the power spectra themselves. Our primary interest was to model differences in connectivity within a cortical hierarchy defined *a priori* that best explained observed differences in power spectra. We focus on the DCM of induced responses so that we can include information from cross frequency coupling, which is an important means of inter-regional information transfer between hierarchically related regions of cortex.<sup>30</sup> DCM of the ERP<sup>25</sup> was used as a secondary analysis to confirm the findings using a very different, biologically plausible model.

### Dynamic causal modelling of induced responses

For a thorough description of DCM of time–frequency responses, see Chen and colleagues<sup>25,31</sup> In brief, DCM of induced responses models the temporal evolution of instantaneous power in a source as a function  $f(\cdot)$  of power in all sources. The equation for the model is as follows, where  $g(\omega)_i$  is the spectral density, over frequency  $\omega$ , of the  $i$ th unit:

$$\dot{g}(\omega)_i = \sum_j f[g(\omega)_i, g(\omega)_j]$$

This model explains the relationship between the amplitude of an oscillation in one region with that in another. DCM utilises a generalised convolution model of the coefficients of the Taylor series expansion of the model above as the output. Causal inference is permitted as this is a ‘functional’ expansion where time information is retained so we know that the relevant inputs precede the outputs. DCM of induced responses therefore models time-dependent changes in spectral energy. Thus, we can model the dynamics of the equation above using a first-order Taylor expansion to give:

$$\tau \dot{g}(t) = \tau \begin{pmatrix} \dot{g}_1 \\ \vdots \\ \dot{g}_J \end{pmatrix} = \begin{pmatrix} A_{11} & \cdots & A_{1J} \\ \vdots & \ddots & \vdots \\ A_{J1} & \cdots & A_{JJ} \end{pmatrix} g(t) + \begin{pmatrix} C_1 \\ \vdots \\ C_J \end{pmatrix} u(t)$$

In this context, the matrices  $A$  and  $C$  contain coupling parameters that explain changes in spectral activity at each node based on spectral changes in all nodes and inputs  $u(t)$ , that is TMS pulses, to the model.  $A$  and  $C$  can be further defined:

$$A_{ij} = \begin{pmatrix} a_{ij}^{11} & \cdots & a_{ij}^{1K} \\ \vdots & \ddots & \vdots \\ a_{ij}^{K1} & \cdots & a_{ij}^{KK} \end{pmatrix} \quad C_i = \begin{pmatrix} C_i^1 \\ \vdots \\ C_i^K \end{pmatrix}$$

The scalar  $a_{ij}^{kl}$  relays how changes in the  $k$ th frequency in the  $i$ th source depend on the  $l$ th frequency in the  $j$ th source. Similarly,  $c_i^k$  explains the frequency-specific influence of the TMS input on the  $k$ th frequency of the  $i$ th source. Together this allows modelling of ‘within frequency’ and ‘cross-frequency’ coupling, ‘within’ (i.e. self modulation) and ‘between’ sources.

The spatial forward model embedded in our DCM models for induced responses used a head model computed using the boundary element method, with homogeneous and isotropic conductivity as an approximation to the brain, cerebrospinal fluid (CSF), skull, and scalp surfaces. Co-registration of electrode position and the head model was performed in each subject before model computation. Cortical sources were modelled as equivalent current dipoles (ECDs)<sup>25,36</sup> centered on coordinates of six cortical sources that were selected *a priori* based on their hierarchical connectivity with the occipital lobe.<sup>26,27</sup> Source locations (and coordinates) were: left inferior occipital gyrus (IOG) (MNI  $-27-97-10$ ), right IOG ( $27-97-10$ ),

left superior parietal lobule (SPL) ( $-26-64-56$ ), right SPL ( $26-64-56$ ), left dorsolateral prefrontal cortex (PFC) ( $-48-40-20$ ), and right dorsolateral PFC ( $48-40-20$ ).

### Bayesian model selection for induced responses

For the DCM analysis of induced responses, individual TMS-EEG trials were linearly detrended and BMS was used to optimise model parameters for the analysis, with both awake and propofol data included together for selection of parameters. BMS calculates the evidence for a model by taking the marginal likelihood over the conditional density of the model parameters and estimating the probability of the data, given a particular model. This can be used to compare and select the best model amongst alternative models. BMS was performed in a sequential manner to assess parameters for optimal onset time for the DCM of cortical response to TMS (testing 0–20 ms onset times after TMS to 400 ms after TMS; data not shown); the modulation of feedforward connections, feedback connections, or both (Supplementary Fig. S1); the presence of connectivity modulation at lower cortical hierarchy levels, higher cortical hierarchy levels, or both (so-called ‘B parameters’; Supplementary Fig. S2); the presence of linear effects, non-linear (cross-frequency) effects, or both (Supplementary Fig. S3); and inclusion of ‘within region’ intrinsic (self) modulation at each source (Supplementary Fig. S4). The model with the highest posterior probability for each class of model parameter was selected for model comparison in the next step. The best DCM model was kept for the final analysis that compared connectivity parameters between wakefulness and propofol sedation.

### Dynamic causal modelling of the evoked response potential

In contrast to DCM of induced responses, DCM of ERPs focuses on the time domain and aims at finding differences in cortical connectivity best explaining dynamical differences in scalp evoked responses. It also includes a generative model of cortical activity in the form of a neural mass model with dynamic interactions between inhibitory and excitatory subpopulations of neurones within each cortical area, and asymmetries feedforward vs feedback connections that reflect known asymmetries in connectivity between hierarchically related cortical areas.<sup>37</sup> This model is based on three subpopulations<sup>38</sup> of cells: excitatory spiny stellate interneurons, inhibitory interneurons, and pyramidal cells. Within each region, pyramidal cells are bidirectionally coupled to excitatory and inhibitory interneurons, and inhibitory interneurons connect to each other. Pyramidal cells are also the projection neurons, connecting laterally to all three populations of cells in other columns, and to higher and lower levels of the cortical hierarchy. Feedforward projections from pyramidal cells terminate on excitatory interneurons, whereas feedback projections terminate on pyramidal cells and inhibitory interneurons. State equations for DCM of ERPs are explained in detail here.<sup>39</sup>

In this neural mass model, spiny stellate excitatory interneurons act as the recipient cell for exogenous inputs  $u(t)$  (in our case, TMS applied to left IOG). The external input comprises two components. The first input component corresponds to an event-related burst delayed relative to stimulus onset, and is modelled as a gamma density function truncated to peri-stimulus time. The second component models fluctuations in input as a discrete cosine set as a function of peri-stimulus time. Modulatory effects of experimental factors



(e.g. awake vs anaesthetised) are modelled through changes in connection strengths that explain differences in TMS-evoked ERP.

Similar to BMS analysis of DCM for induced responses, BMS for DCM of ERPs was performed in a sequential manner to optimise the onset time of the cortical response to TMS (testing 0–20 ms after TMS); modulation of feedforward connections, feedback connections, or both; and the presence of connectivity modulation at lower cortical hierarchy levels, higher cortical hierarchy levels, or both. For DCM of the ERP, the spatial forward model was parameterised using a boundary element method and the same priors on cortical sources as described above. For DCM of ERPs, a choice between ECD and cortical patches is available<sup>25,36</sup>; BMS revealed higher model evidence for DCM models using cortical patches, which we used in our final model.

### Statistical analysis of dynamic causal modelling estimates for induced responses

Parameter estimates of changes in connectivity between wakefulness and propofol sedation (B parameters) obtained from the Bayes-optimal DCM model were entered in a full factorial design with eight levels (one per connection) and three factors: feedback vs feedforward directions, lower (occipital to parietal) vs higher (parietal to frontal) hierarchical levels, and left vs right hemispheres. First, an omnibus F-contrast investigated for any effect of modulation of cortical connectivity between wakefulness and propofol sedation (using an eye(8) F-contrast as implemented in SPM;  $n=8$  per group). A further F-test searched for an effect of hierarchical level on connectivity changes ( $n=8$  per group). A sensitivity F-test was conducted comparing mild sedation to deep sedation with propofol ( $n=3$  per group). Finally, *post hoc* t-tests investigated the presence of increased vs decreased cross-frequency coupling in feedforward or feedback connections in propofol compared to wakefulness ( $n=8$  per group): two contrasts used zeros for all feedback connections and 1 or -1 for feedforward connections, and two other contrasts used zeros for all feedforward connections and 1 or -1 for feedback connections. The final *post hoc* analyses used a -1 per connection and zeros for all other connections. All results were corrected for multiple comparisons across frequencies using peak-based FWE  $P<0.05$  of the peak response. Where appropriate further exploratory analyses were conducted with  $P<0.001$  of the peak response.

### Statistical analysis of dynamic causal modelling estimates for the evoked response potential

As in DCM of induced responses, parameter estimates for changes in connectivity induced by propofol (compared to awake) were obtained from the 'B parameters' of DCM models. One sample t-tests were then conducted with a null hypothesis of zero change (mean values of 0). Statistical significance was set as a Bonferroni corrected P value of  $0.05/8=0.00625$  (multiple correction for the eight connections (connectivity estimates) tested).

## Results

### Propofol induces a loss of induced and evoked power in EEG responses within single electrodes

We confirmed that changes in induced and evoked power were evident in sensor space. Decreased induced power was

noted in occipital, parietal, and frontal channels after occipital TMS (Fig. 1). Notably, in the occipital channel PO3 30–38 Hz power was reduced (cluster FWE  $P<0.001$ , peak level FWE  $P=0.062$ ). Of the parietal channels, CP3 showed significant differences at 18 Hz (cluster level FWE  $P=0.011$ , peak level FWE  $P=0.215$ ). FWE corrected differences were noted in both frontal channels at 38–40 Hz (AF1 FWE cluster  $P<0.001$ , FWE peak  $P=0.205$ ; AF2 FWE cluster  $P<0.001$ , FWE peak  $P=0.081$ ).

To provide an alternative description of the time frequency changes, we conducted an analysis of evoked power. Decreased evoked power was observed in most electrodes during propofol compared to wakefulness (Fig. 1). In particular, occipital channels PO3 and PO4 showed decreased power respectively at 11 Hz (peak level FWE  $P=0.0127$ ) and 21 Hz (peak level FWE  $P=0.045$ ). In parietal regions, channel CP3 showed decreased evoked power at 12 Hz (peak level FWE  $P=0.017$ ) and 18 Hz (peak level FWE  $P=0.020$ ), and channel CP4 showed decreased power at 29 Hz (peak level FWE  $P=0.034$ ) and 33 Hz (peak level FWE  $P=0.044$ ). Frontal channel AF1 also showed decreased 40 Hz evoked power (peak level FWE  $P=0.045$ ). In summary, induced power changes occurred across channels in the beta and gamma range and, consistent with prior data of the natural frequencies of different brain regions after TMS,<sup>40</sup> the evoked power differences observed over occipital and parietal cortex were in the alpha and beta frequencies, and a peak in the frontal cortex in gamma frequencies.

### Bayesian model selection: dynamic causal modelling of induced responses

To investigate the optimal parameters to include in the DCM, BMS was undertaken. Maximum model evidence was obtained for the following parameter choices: onset time of cortical responses=0 ms (rather than 4, 8, 16, or 20 ms), modulation of both feedforward or feedback connections rather than only one connection type (Fig. 2A), modulation of both occipitoparietal and frontoparietal connections rather than only one cortical hierarchical level (Fig. 2B), both linear and non-linear connectivity vs linear only or non-linear only (Fig. 2C), and intrinsic (self) modulation at each source (Fig. 2D). Critically, within the resulting model, including 0 ms onset time, modulation of all hierarchical levels and connection types and both linear and non-linear power connectivity was given the highest posterior evidence. The best performing model showed a difference in the mean log Bayes factor between groups of 779 (with each subject showing a difference of greater than 3; a difference greater than 3 is considered strong evidence<sup>41</sup>) with the next highest performing model. The optimal model is displayed in Figure 2E, with the connections numbered in the order used in subsequent figures.

### Dynamic causal modelling of induced responses: propofol reduces feedforward connectivity

An example of the awake and propofol source reconstructed and final DCM model data are shown in Supplementary Figure S5. We used a full factorial design to analyse the connectivity changes predicted by DCM, including linear and non-linear frequency relationships, during propofol-induced unresponsiveness compared to wakefulness ( $n=8$  subjects per group). In the DCM, linear connectivity relationships would occur between specific frequencies (e.g. 8 to 8 Hz coupling) whereas non-linear

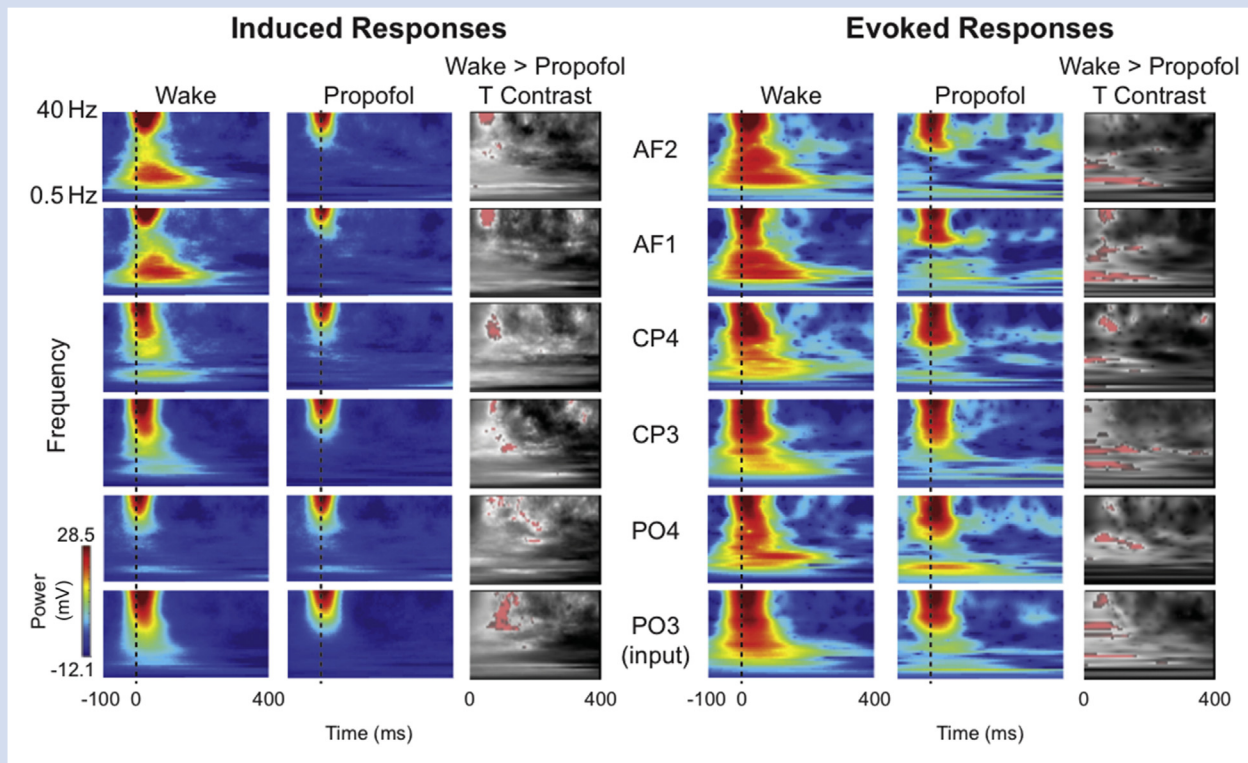


**Fig 1.** Sensor-space induced (left) and evoked (right) EEG responses to transcranial magnetic stimulation (TMS) in wakefulness and propofol: displayed for frontal electrodes AF1 and AF2, parietal electrodes CP3 and CP4 and occipital electrodes PO3 (input, i.e. closest to TMS pulse) and PO4 shown in rows. The columns show the wake and propofol time frequency responses at the respective electrodes from  $-100$  to  $400$  ms after the TMS and in the last column the T contrast results for the propofol-induced decreases in TMS-EEG evoked power between  $0$  to  $400$  ms after TMS. Red implies decreased power during propofol compared to wakefulness (thresholded at  $P < 0.001$  uncorrected for display purposes to show changes for each electrode;  $n = 8$  subjects per group).

connectivity refers to cross-frequency coupling (e.g.  $8-40$  Hz). An omnibus  $F$ -test revealed that propofol-induced unconsciousness was associated with altered theta–theta and theta/alpha–gamma coupling. **Figure 3A** shows statistically significant differences in frequency–frequency coupling between awake and propofol. In the theta band, coupling from peak frequencies at  $8$  to  $8$  Hz was altered by propofol (peak level FWE  $P = 0.029$ ; **Fig. 3B** shows the contrast estimates per connection). Theta/alpha–gamma coupling from  $8$  to  $40$  Hz (peak level FWE  $P = 0.008$ ; **Fig. 3C**) and  $12-38$  Hz (peak level FWE  $P = 0.015$ ; **Fig. 3D**) was also reduced. These connectivity changes predominantly involved feedforward connectivity. A second peak, involving feedforward and feedback connectivity, narrowly missed statistical significance (from  $24$  to  $16$  Hz,  $P < 0.001$  uncorrected corresponding to a peak level FWE  $P = 0.097$ ). Although this model did not have the highest posterior evidence in BMS, we confirmed similar findings with modelling from  $20$  to  $400$  ms, excluding any effect of the TMS artifact ( $n = 8$  subjects per group). We next conducted a sensitivity analysis comparing the available data from three subjects with light sedation from propofol and the more deeply sedated state (Ramsay  $5-6$ ;  $n = 3$  subjects per group). Using the same omnibus  $F$ -test, deeper sedation with propofol was associated with reduced alpha–gamma coupling ( $10-38$  Hz) that again predominantly involved feedforward connections (**Fig. 3E** and **F**).

### Post hoc analyses

Subsequent *post hoc*  $t$ -contrasts of the DCM data for induced responses, which analyse for frequency changes associated with feedforward or feedback processing, identified significant decreases in connectivity under propofol sedation compared to wakefulness in both feedforward and feedback directions (all  $n = 8$  subjects per group). Feedforward connectivity was decreased between alpha to gamma [ $12-38$  Hz; peak level FWE  $P = 0.000$ ; contrast estimate, mean (standard deviation),  $1.04$  ( $0.48$ )]. Meanwhile, feedback connectivity was decreased in the beta range [ $26-32$  Hz; peak level FWE  $P = 0.022$ ; contrast estimate  $0.44$  ( $0.30$ ); and  $22$  to  $14$  Hz; peak level FWE  $P = 0.049$ ; contrast estimate  $0.20$  ( $0.14$ )] and in the alpha range [ $10-12$  Hz; peak level FWE  $P = 0.029$ ; contrast estimate  $0.27$  ( $0.19$ )].

In order to identify which connections were involved in these changes, we performed *post hoc* T contrasts over each connection (**Fig. 4**). All feedforward connections showed depressed connectivity induced by propofol: left IOG to SPL [connection 1:  $12-36$  Hz; contrast estimate:  $0.62$  ( $0.36$ ), peak level FWE  $P = 0.009$ ], right IOG to SPL [connection 2:  $6-40$  Hz; contrast estimate:  $0.29$  ( $0.17$ ), peak level FWE  $P = 0.004$ ], left SPL to PFC [connection 3:  $8$  to  $8$  Hz; contrast estimate:  $0.19$  ( $0.11$ ), peak level FWE  $P = 0.018$ ], right SPL to PFC [connection 4:  $8-40$  Hz; contrast estimate:  $0.19$  ( $0.11$ ), peak level FWE  $P = 0.030$ ]. One feedback connection, right SPL to IOG, also exhibited

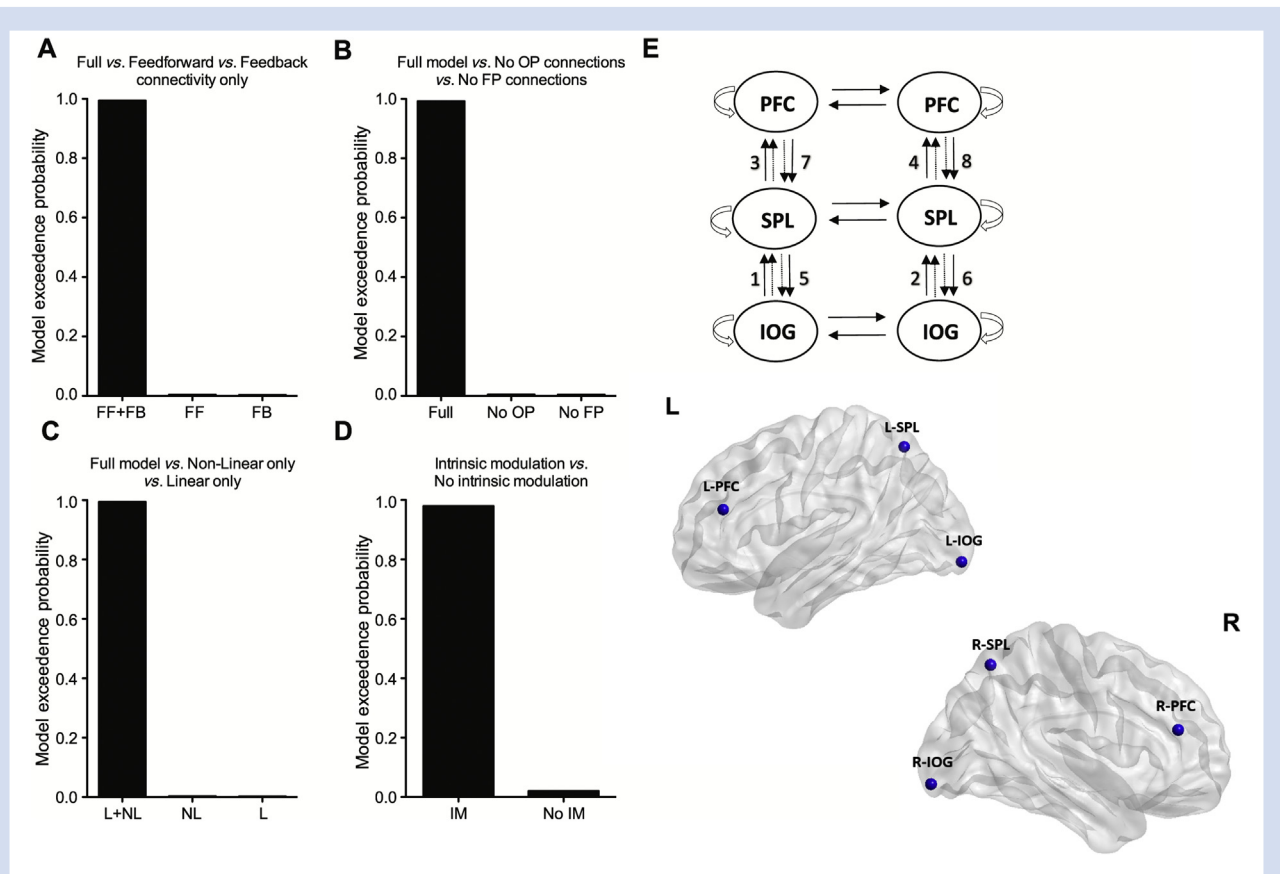


**Fig 2.** Bayesian model selection for the dynamic causal models with different connectivity modulation profiles. (A) Full model vs feedforward connections only vs feedback connections only (as shown in [Supplementary Fig. S1](#)) and (B) full model vs full with no occipitoparietal connections vs full with no frontoparietal connections (as shown in [Supplementary Fig. S2](#)); (C) full model vs non-linear cross-frequency coupling (e.g. 8–30 Hz) vs linear (e.g. 8 to 8 Hz coupling) coupling modulations (as shown in [Supplementary Fig. S3](#)) and (D) inclusion of intrinsic modulation at the source or not (as shown in [Supplementary Fig. 4A](#)). The optimal DCM selected after BMS is shown in (E). Numbers 1–8 in (E) refer to connection order for parameter estimates as displayed in [Figures 2 and 3](#). BMS, Bayesian model selection; DCM, dynamic causal modelling; FB, feedback; FF, feedforward; FP, frontoparietal; IM, intrinsic modulation; IOG, inferior occipital gyrus; L, linear; NL, non-linear; OP, occipitoparietal; PFC, prefrontal cortex; SPL, superior parietal lobule. Arrows indicate linear coupling, dashed arrows denote non-linear coupling. The anatomical locations are presented on a template brain showing left (L) and right (R) hemispheres. Based on  $n=8$  subjects per group.

depressed connectivity in various frequency bands [connection 6: 8 to 8 Hz: contrast estimate: 0.14 (0.08), peak level FWE  $P=0.014$ ; 40 to 20 Hz: contrast estimate: 0.20 (0.14), peak level FWE  $P=0.031$ ; and 26–36 Hz: contrast estimate: 0.16 (0.11), peak level FWE  $P=0.043$ ].

### Dynamic causal modelling for evoked response potentials: propofol reduces feedforward connectivity

DCM for ERPs included a three subpopulation neural mass model at each cortical source<sup>38</sup> ([Fig. 5A](#)) that is not part of the DCM for induced responses. The final model selected by BMS is shown in [Figure 5B](#) with an example of the model applied to a single subject ERP in [Supplementary Figure S6](#). DCM of the ERP demonstrated a similar emphasis on the suppression of feedforward signalling during propofol-induced unresponsiveness ([Fig. 5C](#)). After Bonferroni correction for multiple comparison across eight connections tested, only the feedforward connection contrast estimate from left IOG to SPL showed significant impairment after left-sided occipital TMS

( $P=0.004$ ). A qualitatively similar result was obtained with modelling from 20 to 400 ms after TMS, revealing the affected connection was feedforward left occipital to parietal; however, this did not reach significance at  $P<0.00625$  ( $P=0.007$ ).

## Discussion

Propofol diminished evoked power after TMS across several sensors, with some variation in these sensors dependent on the underlying hierarchical regions of cortex. DCM of induced responses and ERPs after occipital TMS demonstrated impaired feedforward connectivity during propofol-induced unresponsiveness. Herein, we formally describe the diminished propagation of cortical responses after TMS targeted to a lower-order cortical region.<sup>1,2,5</sup> This manifested as predominantly impaired feedforward connectivity, although feedback changes were also apparent in *post hoc* testing. This is important as the anaesthesia literature focuses heavily on feedback signalling. Our parsimonious explanation is that both feedback and feedforward

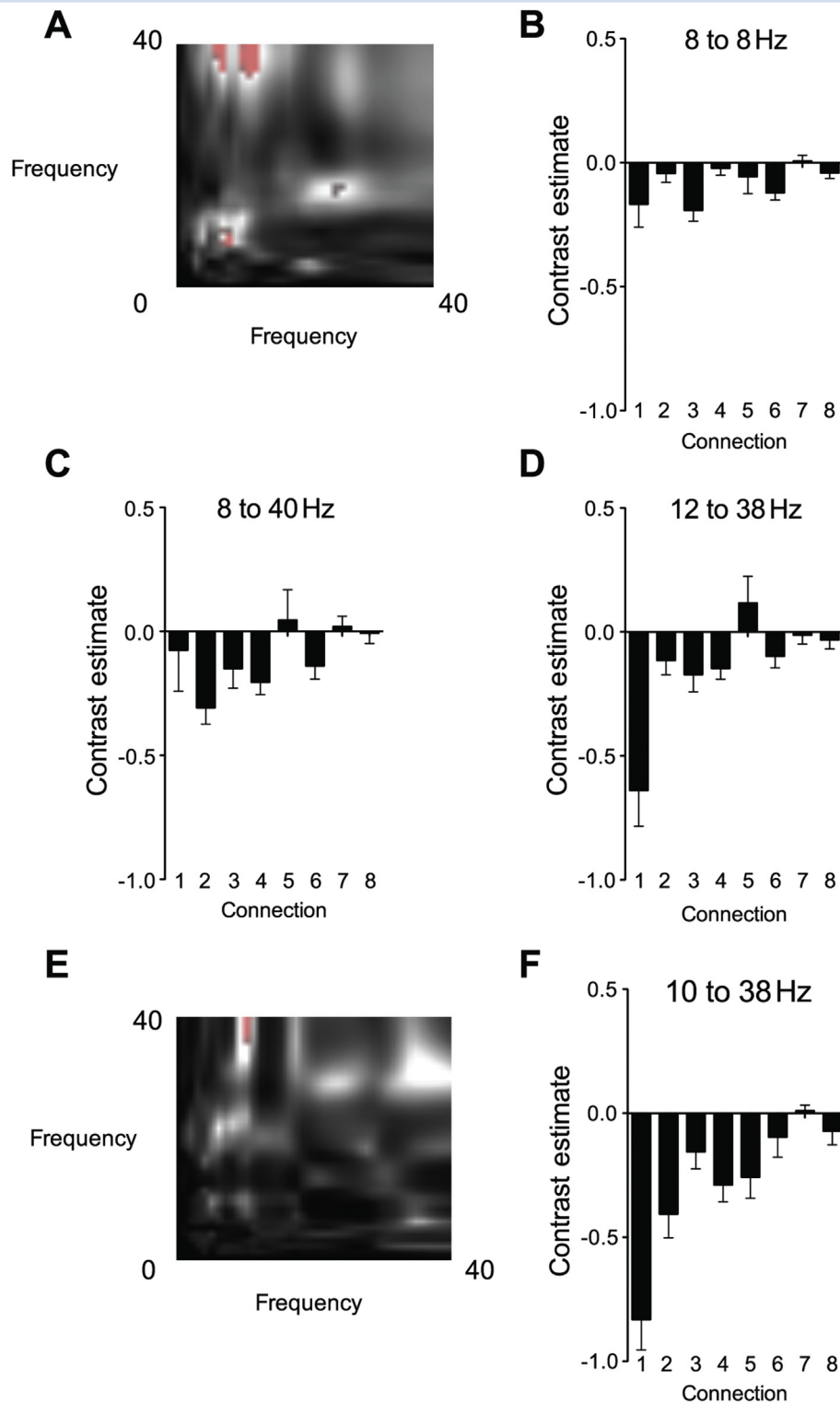


**Fig 3.** Decreased cross-frequency coupling throughout the cortical hierarchy during propofol-induced unconsciousness. (A) Frequency vs frequency plot displaying the significant clusters of altered cross-frequency coupling revealed by omnibus F-test in red. (B) Parameter estimates for change in connectivity strength over connections 1–8 for propofol compared to wakefulness, for the maximum peaks of significance plotted in (A): 8–8 Hz (B), 8–40 Hz (C), and 12–38 Hz (FWE  $P < 0.05$ ;  $n = 8$  subjects per group). (E) and (F) show the sensitivity analysis comparing the difference in mild sedation (Ramsay scale 3) compared to deep sedation (Ramsay scale 5–6;  $n = 3$  subjects per group). (E) Frequency vs frequency plot displaying the significant clusters of altered cross-frequency coupling revealed by omnibus F-test in red for the mild vs deep sedation. (F) Parameter estimates for change in connectivity strength over connections 1–8 for propofol compared to wakefulness, for the maximum peaks of significance plotted in (E) at 10–38 Hz coupling (FWE  $P < 0.05$ ). FWE, family-wise error.



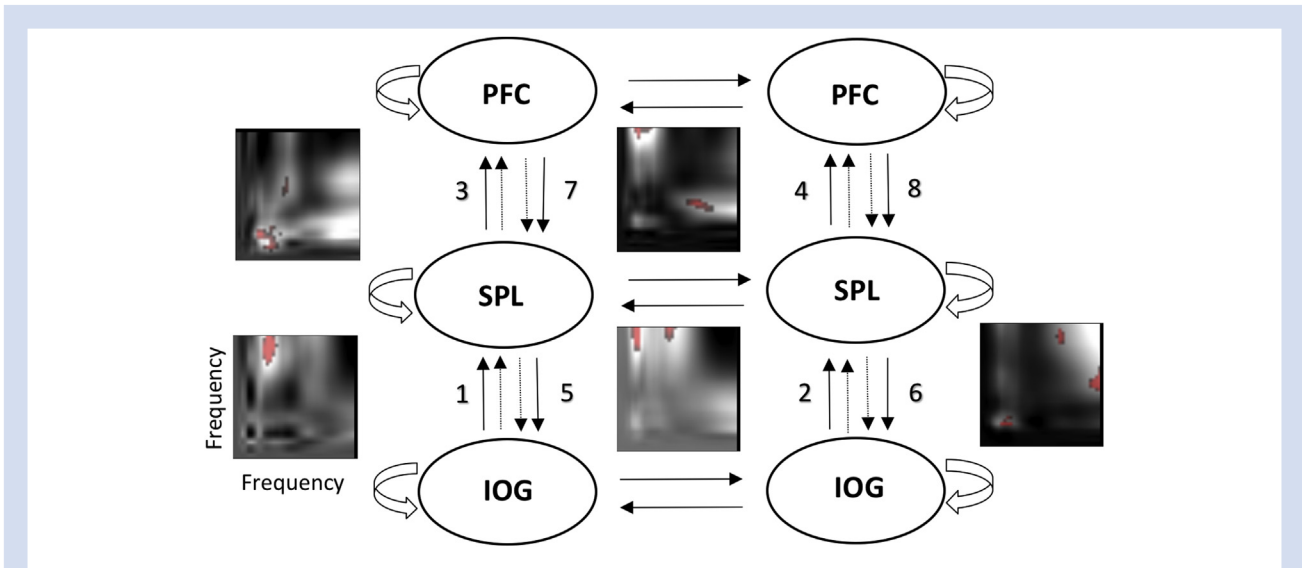


**Fig 4.** Post hoc T contrasts show that propofol impairs connectivity in five out of eight connections in DCM of the induced response. Across the eight connections between inferior occipital gyrus (IOG), superior parietal lobule (SPL) and PFC (prefrontal cortex), five connections show significant differences in T contrasts (connections 1–4 and 6). For each connection where family-wise error (FWE) corrected differences ( $P < 0.05$ ) were detected, a frequency–frequency plot is shown (to the left of the connection number for plots 1–4 that show feedforward connections) and to the right of connection number 6, a feedback connection). Red denotes significant impairments frequency coupling for that connection (FWE  $P < 0.05$ ). Arrows indicate linear coupling, dashed arrows denote non-linear coupling. Based on  $n = 8$  subjects per group.

connectivity are impaired under anaesthesia, and each form is more easily revealed in different paradigms (resting state vs TMS evoked responses from lower order cortex). This is biologically plausible as resting state measures may

emphasise feedback connectivity,<sup>16,29,42</sup> whereas evoked responses recruit feedforward pathways.<sup>23,43</sup> BMS identified a model with both feedforward and feedback connections as best explaining the data, supporting our intention to

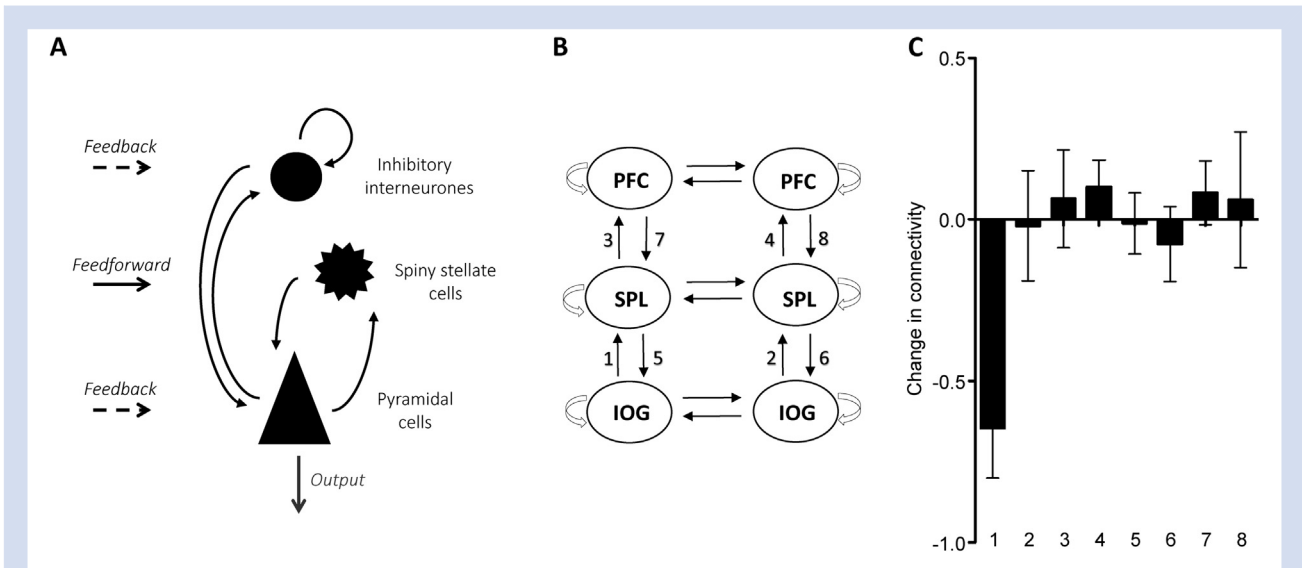


**Fig 5.** Propofol impairs feedforward coupling in a dynamic causal model of the evoked response potential (ERP). (A) Displays the cortical microcircuitry assumed at each source in the biophysical DCM model for the ERP (that is not included for DCM of induced responses). The responses of superficial and deep pyramidal cells (triangles) are modulated by spiny stellate cells and inhibitory interneurons. (B) The final model selected by BMS. (C) Parameter estimates for change in connectivity strength for connections 1–8 for propofol compared to wakefulness. Connection 1 (feedforward from left IOG to left SPL) shows significantly impaired connectivity (Bonferroni corrected  $P < 0.05$ ). Based on  $n = 8$  subjects per group. BMS, Bayesian model selection; DCM, dynamic causal modelling; IOG, inferior occipital gyrus; SPL, superior parietal lobule; PFC, prefrontal cortex.

sensitively test bidirectional effects on connectivity in the cortical hierarchy.

BMS of DCM suggested that the most complex model, including both within and cross-frequency coupling, and in feedback and feedforward directions, best explained our data. This means that effects on feedback and feedforward connections could be sensitively tested in our experiment. From this basis, we investigated the impact of propofol titrated to induce unresponsiveness, identifying predominantly an effect on feedforward connectivity. TMS, which is a direct cortical stimulus that bypasses any subcortical gate for signalling, is an artificial stimulus that lacks a biological analogue. As such, the biological relevance of the stimulus may be questioned. However, TMS provides direct information about cortical processing<sup>1,2,4,5</sup> and has been used successfully across cognitive neuroscience to this end. Furthermore, TMS has remarkable diagnostic value to differentiate levels of consciousness<sup>1</sup>; we propose that understanding the cortical response to TMS will provide novel insights into the mechanisms of consciousness.

### Caveats

We have reported that 27% of subjects report dreaming on awakening from multimodal clinical anaesthesia with propofol.<sup>44</sup> In this volunteer study, no subjects (0/8) reported such experiences. Future larger volunteer studies should identify whether dreaming also occurs in the laboratory setting. Of many methods of investigating connectivity, we chose to use DCM based on our prior experience<sup>16,45</sup> and our focus on modelling effects in the cortical hierarchy as explicitly as possible. All methods of connectivity assessment have potential pitfalls,<sup>46</sup> and DCM has been similarly critiqued.<sup>25,31,47,48</sup> DCM of the induced response does not rely on specific biological priors about the cortical microcircuit, making it less vulnerable to criticism over the specifics of the biological model used in DCM for ERP.<sup>25,31</sup> Both models, however, indicated decreased feedforward connectivity during propofol-induced unconsciousness. We focused on a hierarchy of cortical sources involved in visual perception. Importantly the TMS stimulus did not change conscious experience itself, but did provoke an induced/evoked EEG response that could be used to test changes in connectivity. Similar to the 'gold standard' connectivity measure of Granger causality,<sup>46</sup> the modelling is time dependent, ensuring that inputs precede outputs. A strength over Granger causality analysis is that DCM of induced responses permits inferences about cross-frequency coupling, which are prominent in cortical dynamics.<sup>30</sup> Nonetheless, DCM has weaknesses. It is computationally intensive, even when limited to eight frequency modes. Hence, despite the apparent complexity of our modelling approach, DCM might overlook even more complex—but biologically important—relationships. The primary strength in our approach is to provide a model-driven assessment of connectivity 'between regions' and 'cross-frequencies'. This represents a novel approach for EEG analysis in the anaesthesia literature, which typically uses 'within frequency' connectivity measures for effects 'between regions'.

A further strength of our analysis is the robust statistical approach using FWE correction based on random field theory to reduce type 1 error. We then supported our findings with DCM of the ERP, which uses a biological model based on the canonical cortical microcircuit.<sup>23,38,49</sup> These models have proved useful for probing conscious and unconscious states,<sup>45</sup>

and our use of this biological model supports the effect on feedforward processing elucidated by DCM of induced responses. It is also important to note that DCM of ERPs (compared to the induced model) invoked a different spatial forward model, providing further evidence that the results from DCM of the induced response are robust.

Although the focus of our study was to identify whether propofol interfered with connectivity, including cross-frequency coupling, our scalp EEG recordings are not well suited to detect effects on ascending connectivity within higher gamma frequencies.<sup>50</sup> Future studies should use alternate methodologies, for example magnetoencephalography or intracranial recordings, to assess the role of high gamma activity. Also, investigating the role of the thalamus, although of potential theoretical interest<sup>6,51</sup> was not technically feasible in the present study, but could be investigated in future studies particularly using invasive recordings.

A further important caveat is that our awake data were collected with eyes open, whereas during our sedation data subjects had their eyes closed. Although seemingly a small detail, in spontaneous EEG eye opening and closing is associated with changes in occipital cortical alpha power, which could have affected the results. As this may have affected the results, we conducted a sensitivity analysis of the available data (three subjects) who had TMS data collected at Ramsay sedation scale 3 compared with level 5 to 6 ( $n=3$  subjects per group; Fig. 3E and F). At both these stages of sedation, subjects had their eyes closed. These data support the primary endpoint showing that alpha–gamma coupling, predominantly in feedforward connections, is affected by propofol at the transition to loss of responsiveness to the environment. Hence, we consider it unlikely that the changes in the power coupling of the induced response that we observe relate merely to the eyes being open or closed and the consequent effects on the spectra of occipital cortex. It is worth stressing that we treated the awake and propofol sedation periods as steady state, but the propofol period may not have reached a steady state with a 5 min equilibration. Hence the periods of propofol sedation may be more unstable than would be ideal.

### Implications for understanding impairment of consciousness induced by anaesthetics

We have shown reduced power responses under propofol after TMS at several cortical electrodes. If this is shown in other paradigms to track levels of consciousness, a monitor might be derived that looks at reduced power responses at a single electrode. This hypothesis will need testing in further volunteers before clinical trial testing begins. Fundamentally we show that feedforward signalling is impaired under anaesthesia. Critically this involved theta–theta and theta/alpha–gamma coupling, which prior studies have suggested are critical to feedforward processing.<sup>23,43,46,52</sup> These findings complement prior work showing that propofol impairs long-range cortical connectivity<sup>16,53,54</sup> and that feedforward and feedback connections are affected in different frequency bands.<sup>43,50,52,55</sup> To this end, our sensitivity analyses showed feedback changes in the beta and alpha bands that are consistent with the literature. Although general anaesthetics are thought to affect cross-frequency coupling within region<sup>56,57</sup> and phase–amplitude coupling within frontal and parietal electrodes,<sup>12,16,56,58</sup> our results suggest that cross-frequency power coupling between levels of the cortical hierarchy is affected by anaesthesia. Theoretically, this would

affect integration of information across the cortical hierarchy.

Our experiments were designed to identify whether effects on feedforward processing could be detected after TMS by targeting a lower-order cortical region. As such, we maximised sensitivity to identify this feedforward effect. This may have meant that feedback effects only came to prominence after lowering the statistical threshold on the F-test for induced responses or in the *post hoc* t-tests. However, we did not identify a strong signal on feedback processing in DCM of the ERP. Nonetheless, we find it plausible that propofol affects both feedforward and feedback processing; the next stage is to understand the convergence or divergence of these effects during clinical anaesthesia. It is worth emphasising that feedback frontoparietal connectivity was not found to be affected by propofol unlike in our prior DCM study.<sup>16</sup> Rather, feedback SPL to IOG connectivity was impaired. This may relate to the specifics of our experimental paradigm (TMS targeted to the lower-order cortex), and this should be tested through TMS applied to higher-order regions to more directly recruit feedback frontoparietal connectivity.

A recent study showed that ~5% of patients may be aware of sensory stimuli ('connected consciousness') under general anaesthesia, which is a potentially important clinical problem<sup>6,59</sup> that likely involves ascending transmission of sensory information. As sensory cortices are still readily activated by surgical stimulation under anaesthesia,<sup>6</sup> and connected consciousness can occur under anaesthesia without frontal cortical activation,<sup>60</sup> future studies should assess how anaesthesia affects feedforward connectivity after evoked sensory stimuli and what levels of the cortical hierarchy are involved. In particular, we hypothesise that impaired feedforward connectivity contributes to sensory disconnection from the environment.<sup>6</sup> Further experiments recording TMS-EEG during states of both unconsciousness and of connected/disconnected consciousness would elucidate if loss of hierarchical cross-frequency coupling within the cortex also contributes to anaesthesia-induced sensory disconnection. Nonetheless, bidirectional effects on hierarchical connectivity are altered during propofol-induced loss of consciousness, furthering our understanding of cortical connectivity as probed by TMS.

## Conclusions

Our results suggest that cortical time–frequency spectral responses to TMS are perturbed by propofol sedation. Impaired feedforward connectivity, using cross-frequency coupling between hierarchical cortical regions, is evident during propofol-induced unconsciousness. These results shed light on the neural mechanisms of the loss of integration induced by propofol sedation in the cerebral cortex, and suggest that changes in both feedforward and feedback connectivity throughout the cortical hierarchy might be involved in the effect of anaesthesia on consciousness.

## Authors' contributions

Research design: R.D.S., M.D., J.S., R.M., A.R., M.I.B., M.B.  
Data analysis: R.D.S., M.D., J.S., R.M., A.R., M.I.B., M.B.  
Writing paper: R.D.S., M.D., J.S., R.M., A.R., M.I.B., O.G., M.A.B., M.R., M.M., S.L., G.T., M.B.  
Research: O.G., M.A.B., V.B., J.F.B., M.R., M.M., S.L., M.B.

## Declaration of interest

VB: unrestricted grant from Orion Pharma of about €30 000, editor-in-chief of *Acta Anaesthesiologica Belgica*. GT: unrestricted grant funding from Philips Healthcare and serves on the advisory board of the Allen Institute for Brain Science.

## Funding

RDS, MD, AR and MIB are supported by the Department of Anesthesiology, University of Wisconsin. RDS is supported by the National Institutes of Health (NIH) grant K23 AG055700 (Bethesda MD, USA). MIB is supported by NIH grant R01 GM109086. MR is partially supported by Grant 'Giovani Ricercatori' GR-2011-02352031 from the Italian Ministry of Health. MM is supported by James S. McDonnell Foundation Scholar Award 2013 and EU grant H2020 agreement 720270-Human Brain Project SGA1. MB is supported by NIH grant R03NS096379. GT is supported by NIH/NCCAM P01AT004952 and NIH/NIMH 5P20MH077967. OG a postdoctoral fellow and SL a research director at the national fund for scientific research (FNRS). This research was supported by the Belgian National Funds for Scientific Research (FNRS), Human Brain Project (EU-H2020-FETFLAGSHIP-HBP-SGA1-GA720270), Luminous project (EU-H2020-FETOPEN-GA686764), the European Commission, the James McDonnell Foundation, the Mind Science Foundation, the French Speaking Community Concerted Research Action (ARC-06/11-340), and the University and University Hospital of Liège.

## Appendix A. Supplementary data

Supplementary data related to this article can be found at <https://doi.org/10.1016/j.bja.2018.07.006>.

## References

- Casali AG, Gosseries O, Rosanova M, et al. A theoretically based index of consciousness independent of sensory processing and behavior. *Sci Trans Med* 2013; 5: 198ra05
- Ferrarelli F, Massimini M, Sarasso S, et al. Breakdown in cortical effective connectivity during midazolam-induced loss of consciousness. *Proc Natl Acad Sci U S A* 2010; 107: 2681–6
- Massimini M, Ferrarelli F, Huber R, Esser SK, Singh H, Tononi G. Breakdown of cortical effective connectivity during sleep. *Science* 2005; 309: 2228–32
- Rosanova M, Gosseries O, Casarotto S, et al. Recovery of cortical effective connectivity and recovery of consciousness in vegetative patients. *Brain* 2012; 135: 1308–20
- Sarasso S, Boly M, Napolitani M, et al. Consciousness and complexity during unresponsiveness induced by propofol, xenon, and ketamine. *Curr Biol* 2015; 25: 3099–105
- Sanders RD, Tononi G, Laureys S, Sleigh JW. Unresponsiveness ≠ unconsciousness. *Anesthesiology* 2012; 116: 946–59
- Tononi G, Boly M, Massimini M, Koch C. Integrated information theory: from consciousness to its physical substrate. *Nat Rev Neurosci* 2016; 17: 450–61
- Tononi G. An information integration theory of consciousness. *BMC Neurosci* 2004; 5: 42
- Imas OA, Ropella KM, Ward BD, Wood JD, Hudetz AG. Volatile anesthetics disrupt frontal–posterior recurrent information transfer at gamma frequencies in rat. *Neurosci Lett* 2005; 387: 145–50

10. Peltier SJ, Kerstens C, Hamann SB, Sebel PS, Byas-Smith M, Hu X. Functional connectivity changes with concentration of sevoflurane anesthesia. *Neuroreport* 2005; **16**: 285–8
11. Alkire MT. Loss of effective connectivity during general anesthesia. *Int Anesthesiol Clin* 2008; **46**: 55–73
12. Lee U, Kim S, Noh GJ, Choi BM, Hwang E, Mashour GA. The directionality and functional organization of frontoparietal connectivity during consciousness and anesthesia in humans. *Conscious Cogn* 2009; **18**: 1069–78
13. Ku SW, Lee U, Noh GJ, Jun IG, Mashour GA. Preferential inhibition of frontal-to-parietal feedback connectivity is a neurophysiologic correlate of general anesthesia in surgical patients. *PLoS One* 2011; **6**: e25155
14. Schrouff J, Perlberg V, Boly M, et al. Brain functional integration decreases during propofol-induced loss of consciousness. *NeuroImage* 2011; **57**: 198–205
15. Liu X, Lauer KK, Ward BD, Rao SM, Li SJ, Hudetz AG. Propofol disrupts functional interactions between sensory and high-order processing of auditory verbal memory. *Hum Brain Mapp* 2012; **33**: 2487–98
16. Boly M, Moran R, Murphy M, et al. Connectivity changes underlying spectral EEG changes during propofol-induced loss of consciousness. *J Neurosci* 2012; **32**: 7082–90
17. Maksimow A, Silfverhuth M, Langsjo J, et al. Directional connectivity between frontal and posterior brain regions is altered with increasing concentrations of propofol. *PLoS One* 2014; **9**: e113616
18. Raz A, Grady SM, Krause BM, Uhlrich DJ, Manning KA, Banks MI. Preferential effect of isoflurane on top-down vs. bottom-up pathways in sensory cortex. *Front Syst Neurosci* 2014; **8**: 191
19. Nelson LE, Guo TZ, Lu J, Saper CB, Franks NP, Maze M. The sedative component of anesthesia is mediated by GABA(A) receptors in an endogenous sleep pathway. *Nat Neurosci* 2002; **5**: 979–84
20. Angel A. The G. L. Brown lecture. Adventures in anaesthesia. *Exp Physiol* 1991; **76**: 1–38
21. Hubel DH, Wiesel TN. Receptive fields, binocular interaction and functional architecture in the cat's visual cortex. *J Physiol* 1962; **160**: 106–54
22. Hubel DH, Wiesel TN. Receptive fields and functional architecture of monkey striate cortex. *J Physiol* 1968; **195**: 215–43
23. Bastos AM, Usrey WM, Adams RA, Mangun GR, Fries P, Friston KJ. Canonical microcircuits for predictive coding. *Neuron* 2012; **76**: 695–711
24. Arnal LH, Giraud AL. Cortical oscillations and sensory predictions. *Trends Cogn Sci* 2012; **16**: 390–8
25. Chen CC, Kiebel SJ, Kilner JM, et al. A dynamic causal model for evoked and induced responses. *Neuroimage* 2012; **59**: 340–8
26. Dentico D, Cheung BL, Chang JY, et al. Reversal of cortical information flow during visual imagery as compared to visual perception. *Neuroimage* 2014; **100**: 237–43
27. Ganis G, Schendan HE. Visual mental imagery and perception produce opposite adaptation effects on early brain potentials. *Neuroimage* 2008; **42**: 1714–27
28. Hipp JF, Hawellek DJ, Corbetta M, Siegel M, Engel AK. Large-scale cortical correlation structure of spontaneous oscillatory activity. *Nat Neurosci* 2012; **15**: 884–90
29. Blain-Moraes S, Tarnal V, Vanini G, et al. Neurophysiological correlates of sevoflurane-induced unconsciousness. *Anesthesiology* 2015; **122**: 307–16
30. Canolty RT, Knight RT. The functional role of cross-frequency coupling. *Trends Cogn Sci* 2010; **14**: 506–15
31. Chen CC, Kiebel SJ, Friston KJ. Dynamic causal modelling of induced responses. *Neuroimage* 2008; **41**: 1293–312
32. Ramsay MA, Savege TM, Simpson BR, Goodwin R. Controlled sedation with alphaxalone–alphadolone. *BMJ* 1974; **2**: 656–9
33. Murphy M, Bruno MA, Riedner BA, et al. Propofol anesthesia and sleep: a high-density EEG study. *Sleep* 2011; **34**: 283–91
34. Marsh B, White M, Morton N, Kenny GN. Pharmacokinetic model driven infusion of propofol in children. *Br J Anaesth* 1991; **67**: 41–8
35. Gosseries O, Sarasso S, Casarotto S, et al. On the cerebral origin of EEG responses to TMS: insights from severe cortical lesions. *Brain Stimul* 2015; **8**: 142–9
36. Litvak V, Mattout J, Kiebel S, et al. EEG and MEG data analysis in SPM8. *Comput Intell Neurosci* 2011; **2011**: 852961
37. Felleman DJ, Van Essen DC. Distributed hierarchical processing in the primate cerebral cortex. *Cereb Cortex* 1991; **1**: 1–47
38. David O, Kiebel SJ, Harrison LM, Mattout J, Kilner JM, Friston KJ. Dynamic causal modeling of evoked responses in EEG and MEG. *Neuroimage* 2006; **30**: 1255–72
39. Kiebel SJ, Garrido MI, Moran RJ, Friston KJ. Dynamic causal modelling for EEG and MEG. *Cogn Neurodyn* 2008; **2**: 121–36
40. Rosanova M, Casali A, Bellina V, Resta F, Mariotti M, Massimini M. Natural frequencies of human corticothalamic circuits. *J Neurosci* 2009; **29**: 7679–85
41. Kass RE, Raftery AE. Bayes factors. *J Am Stat Assoc* 1995; **90**: 773–95
42. Lee U, Muller M, Noh GJ, Choi B, Mashour GA. Dissociable network properties of anesthetic state transitions. *Anesthesiology* 2011; **114**: 872–81
43. Bastos AM, Litvak V, Moran R, Bosman CA, Fries P, Friston KJ. A DCM study of spectral asymmetries in feedforward and feedback connections between visual areas V1 and V4 in the monkey. *Neuroimage* 2015; **108**: 460–75
44. Leslie K, Sleigh J, Paech MJ, Voss L, Lim CW, Sleigh C. Dreaming and electroencephalographic changes during anesthesia maintained with propofol or desflurane. *Anesthesiology* 2009; **111**: 547–55
45. Boly M, Garrido MI, Gosseries O, et al. Preserved feedforward but impaired top-down processes in the vegetative state. *Science* 2011; **332**: 858–62
46. Bastos AM, Schoffelen JM. A Tutorial review of functional connectivity analysis methods and their interpretational pitfalls. *Front Syst Neurosci* 2015; **9**: 175
47. Daunizeau J, David O, Stephan KE. Dynamic causal modelling: a critical review of the biophysical and statistical foundations. *Neuroimage* 2011; **58**: 312–22
48. Friston K, Daunizeau J, Stephan KE. Model selection and gobbledygook: response to Lohmann et al. *Neuroimage* 2013; **75**: 275–8. discussion 9–81
49. Pinotsis DA, Moran RJ, Friston KJ. Dynamic causal modeling with neural fields. *Neuroimage* 2012; **59**: 1261–74
50. Fontolan L, Morillon B, Liegeois-Chauvel C, Giraud AL. The contribution of frequency-specific activity to hierarchical information processing in the human auditory cortex. *Nat Commun* 2014; **5**: 4694
51. Alkire MT, Hudetz AG, Tononi G. Consciousness and anesthesia. *Science* 2008; **322**: 876–80



52. Bastos AM, Vezoli J, Bosman CA, et al. Visual areas exert feedforward and feedback influences through distinct frequency channels. *Neuron* 2015; **85**: 390–401
53. Boveroux P, Vanhaudenhuyse A, Bruno MA, et al. Breakdown of within- and between-network resting state functional magnetic resonance imaging connectivity during propofol-induced loss of consciousness. *Anesthesiology* 2010; **113**: 1038–53
54. Lee U, Mashour GA, Kim S, Noh GJ, Choi BM. Propofol induction reduces the capacity for neural information integration: implications for the mechanism of consciousness and general anesthesia. *Conscious Cogn* 2009; **18**: 56–64
55. Furl N, Coppola R, Averbek BB, Weinberger DR. Cross-frequency power coupling between hierarchically organized face-selective areas. *Cereb Cortex* 2014; **24**: 2409–20
56. Li D, Li X, Hagihira S, Sleight JW. Cross-frequency coupling during isoflurane anaesthesia as revealed by electroencephalographic harmonic wavelet bicoherence. *Br J Anaesth* 2013; **110**: 409–19
57. Mukamel EA, Pirondini E, Babadi B, et al. A transition in brain state during propofol-induced unconsciousness. *J Neurosci* 2014; **34**: 839–45
58. Johansen JW, Sebel PS. Development and clinical application of electroencephalographic bispectrum monitoring. *Anesthesiology* 2000; **93**: 1336–44
59. Sanders RD, Raz A, Banks MI, Boly M, Tononi G. Is consciousness fragile? *Br J Anaesth* 2016; **116**: 1–3
60. Gaskell AL, Hight DF, Winders J, et al. Frontal alpha–delta EEG does not preclude volitional response during anaesthesia: prospective cohort study of the isolated forearm technique. *Br J Anaesth* 2017; **119**: 664–73

Handling editor: H.C. Hemmings Jr